CONF-8709192--4

Trends vs. Reactor Size of Passive Reactivity Shutdown and Control Performance

D. C. Wade and E. K. Fujita

CONF-8709192--4

DE88 002939

I) Introduction

The focus of the U.S. advanced reactor program since the cancellation of CRBR has been on inherent safety and cost reduction. The notion is to so design the reactor that in the event of an off normal condition, it brings itself to a safe shutdown condition and removes decay heat by reliance on "inherent processes" i.e. without reliance on devices requiring switching and outside sources of power. Such a reactor design would offer the potential to eliminate costly "Engineered Safety Features", to lower capital costs, and to assuage public unease concerning reactor safety.

For LMR concepts, the goal of passive reactivity shutdown has been approached in the U.S. by designing the reactors for favorable relationships among the power, power/flow, and inlet temperature coefficients of reactivity, for high internal conversion ratio (yielding small burnup control swing), and for a primary pump coastdown time appropriately matched to the delayed neutron hold back of power decay upon negative reactivity input[1]. The use of sodium bonded metallic fuel pins has facilitated the achievement of the passive shutdown design goals as a consequence of their high thermal conductivity and high effective heavy metal density. Alternately, core designs based on derated oxide pins may be able to achieve the passive shutdown features at the cost of larger core volume and increased initial fissile inventory.

For LMR concepts, the passive decay heat removal goal of inherent safety has been approached in U.S. designs by use of pool layouts, larger surface to volume ratio of the reactor vessel with natural draft air cooling of the vessel surface, elevations and redans which promote natural circulation through the core, and thermal mass of the pool contents sufficient to absorb that initial transient decay heat which exceeds the natural draft air cooling capacity.

Two industrial designs using the approaches summarized above have been developed in the USDOE-sponsored LMR innovative design program. The Rockwell International SAFR plant design comprises 4 colocated modules of 350 MWe each while the General Electric PRISM plant design is based on 9 colocated modules of 125 MWe each. Both designs display excellent properties of passive reactivity shutdown and passive decay heat removal. The use of smaller modular units in both concepts has resulted from the reinforcement of three principal design and marketing strategies:

a) the use of larger surface to volume ratio reactor vessels to facilitate passive, natural draft air cooling at the decay heat level,

b) the use of factory fabrication and subsequent barge or rail shipment to the site as a strategy for reducing plant capital cost, and

c) an electrical capacity growth strategy based on sequential addition of small, colocated modules to a plant site so as to better match the electrical capacity growth with the demand as a way to reduce demands on the utility's capital and to reduce its financial risk.

Whereas market environment factors such as items (b) and (c) above are both geographically and temporally variant, the laws of physics upon which the passive reactivity shutdown and passive decay heat removal capabilities of the reactor designs rest presumably are not. Thus, it is of some interest to determine whether or not the inherent safety features displayed by the small modular units can be achieved also in the larger LMR unit sizes typical of LMR programs outside the U.S.

To that end, decay heat removal through natural draft air cooling of the reactor vessel in a pool layout has received some preliminary evaluation which suggests feasibility at larger reactor size[2]. However, irrespective of the eventual outcome of studies regarding the extendability of natural draft air cooling the reactor vessel to larger plant sizes, the use of suitably redundant and diverse DRACS systems[3] offers a potential approach which has no apparent plant rating limit. It remains, then to examine the scaleability with reactor size of the other facet of inherent safety performance i.e. passive reactivity shutdown characteristics. That is the focus of this paper.

II) Reactivity Feedback Parameters which Control Passive Shutdown Characteristics

Reference 1 summarized an approach to evaluating passive reactivity control characteristics based on the use of a quasi-static reactivity balance. Only the main notions will be repeated here, to set the stage for an examination of reactor size effects.

An LMR reactor core can be influenced by external events only through changes in the coolant inlet temperature and flow rate or through externally induced reactivity changes owing to control rod motion or seismically induced core geometry changes. Of these three communication paths, the BOP can influence the core only through coolant inlet temperature. These three all-encompassing paths by which external changes can influence the reactor, are embodied in the three generic ATWS events; Loss-of-Flow without scram (LOF), Loss-of-Heat-Sink without scram (LOHS), and rod runout Transient Overpower (TOP) plus two overcooling accidents: pump overspeed and chilled T_{inlet}. (It is assumed that the reactivity consequences of seismic-induced core geometry changes can always be scoped by an appropriate rod runout TOP initiator and a degradation in radial expansion negative feedback.)

Given the limited ways the core can be influenced by external events, it is useful to write a quasi-static reactivity balance[4] as:

$$0 = \Delta\rho = (P-1)A + (P/F-1)B + \delta T_{in}C + \Delta\rho_{ext} \qquad (1)$$

where P and F are normalized power and flow, δT_{in} is the change from normal coolant inlet temperature, and $\Delta\rho_{ext}$ is the externally-imposed reactivity. Here, A, B, and C are integral reactivity parameters which are measurable on

the operating plant via perturbations introduced through the communication paths*. Here C (¢/°C) is the inlet temperature coefficient of reactivity, (A+B) (¢) is the reactivity decrement experienced in going to full power and flow from zero power isothermal at coolant inlet temperature, B (¢/100% P/F) is the power/flow coefficient, and A is the net (power-flow) (¢) reactivity decrement. In transients which are slow enough to preclude nonequilibrium stored energy in the fuel pins and delayed neutron nonequilibrium, Eq. (1) can be solved for the new power level after inherent adjustment of the reactor core to a new set of externally-controlled conditions of coolant flow, inlet temperature, and externally induced reactivity. The power adjusts up or down to compensate through the power coefficient any reactivity change caused by external events.

When this analysis approach is taken (as discussed in Ref. 1) for all possible external perturbations which the core can experience through these communication paths to the external world; i.e.:

Primary Pump Induced Events (changes in flow)

- LOF
- pump overspeed

Control Rod Induced Events (changes in external reactivity)

- "slow" TOP

BOP Induced Events (changes in inlet temperature)

- LOHS
- chilled inlet temperature,

the asymptotic core outlet temperatures which result from the balance of reactivity, Eq. (1), can be expressed as simple ratios of the measurable integral parameters (see Table I). It is seen in Table I that the asymptotic incremental change in core outlet temperature relative to its normal value (expressed in units of full power steady state coolant temperature rise, ΔT_c) is always determined by three dimensionless ratios of the measurable, integral reactivity parameters; specifically:

A/B
$C\Delta T_c/B$
$\Delta\rho_{TOP}/B$

where

$$\Delta\rho_{TOP} = \left(\frac{\text{Burnup Control Swing}}{\text{No. of Operational Rods}}\right) * \left(\text{1st rod out interaction factor}\right). \quad (2)$$

---

*This measurability is noteworthy in that it provides for a means to monitor the operating plant for the presence of inherent reactivity feedbacks in a range which is known to yield satisfactory passive shutdown performance.

Of all of these unprotected accident scenarios, it is only in the first few tens of seconds of a LOF that the quasi-static reactivity balance is seriously in error. During that short time following initiation of a LOF, the delayed neutron hold back time, $1/\lambda$, of the power decay may be longer than the pump coastdown time, τ, thereby causing a power/flow overshoot which yields a core outlet temperature overshoot relative to the asymptotic value given in Table I. The size of this overshoot can be controlled by choice of the pump time constant, τ; specifically overshoot relative to the asymptote is reduced, the larger is the value of the quantity:

$$\tau\lambda(1 + A/B)^2|B|$$

relative to 1\$.

Examination of Table I shows that all possible unprotected accident scenarios* which are initiated through the three all-encompassing communication paths to the reactor will lead to acceptable asymptotic core outlet temperatures if the following sufficient (but not necessary) ranges for the measurable integral reactivity parameters are met:

$$A/\beta \leq 1$$

$$1 \leq \frac{C\Delta T_c}{B} \leq 2 \qquad (3)$$

$$\frac{\Delta\rho_{TOP}}{|B|} \leq 1$$

A, B, C all negative

and peak overshoot in the LOF will be minimal if:

$$\tau\lambda(1 + A/B)^2|B| > 1\$.$$

Under these conditions, the incremental increase in the outlet temperature above its normal full power, full flow condition never exceeds one ΔT_c.

The set of conditions listed above in Eq. (3) has provided the neutronic design goals for the U.S. LMR modular core designs, and the issue to be addressed here is whether or not they can be achieved in larger LMR cores as well.

---

*The assumptions of the quasi-static approach will be violated in TOP's with periods of a size comparable to or shorter than the fuel pin and fluid time constants -- which are in the range of 1 to 5 sec. Otherwise the above results are general.

III) Trends in Reactivity Feedback Characteristics with Reactor Size

(A) Components of the Integral Reactivity Parameters

Based on their definitions, eg. $C = \left.\frac{\partial \Delta\rho}{\partial T_{in}}\right|_{\text{operating conditions}}$ etc., the integral reactivity parameters A, B, and C can be partitioned into their separate components -- Doppler, radial expansion, etc. The results of this are summarized in Fig. 1. For example, the net (power-flow) decrement, A, is equal to the Doppler plus fuel axial expansion coefficients of reactivity multiplied by the incremental temperature rise of the fuel relative to the coolant*; the dimensions of A is dollars of reactivity, and A ranges in value from 25¢ to $2.00 for current LMR designs. The power/flow coefficient, B, adds to the Doppler and fuel axial expansion coefficients additional terms due to sodium density, above core load pad thermal dilation (i.e. core radial expansion), and control rod driveline expansion+ all multiplied by the average coolant temperature increment relative to the inlet coolant temperature; its dimensions are dollars of reactivity per 100% in power/flow, and the range of values is 25¢ to 75¢ for current LMR designs. The inlet temperature coefficient, C, contains terms due to Doppler, fuel axial expansion, sodium density, and vessel wall+ and grid plate thermal dilation (core radial expansion); its units are $/°C and typical values are about ½ cent/°C.

The separate physical effects themselves depend on reactivity coefficients and material thermal expansion coefficients all appropriately averaged over the relevant temperature distributions in the reactor. For the purposes of these analyses, core-wide reactivity coefficients are used with "average" thermal expansion coefficients appropriate for the temperature ranges throughout the core as defined in Fig. 2. Figure 1 indicates the size ranges of the individual α terms for typical LMR modular cores fueled with mixed oxide and fueled with U/Pu/Zr metal alloy fuels. All α's have units of $/°C and all except α_{Na} are negative.

(B) Trends of the Components with Reactor Size

In order to discern the trends versus reactor size of those reactivity parameter ratios which control passive reactivity shutdown

---

*Whether α_e goes in A or not depends on whether the fuel is free of the clad (fuel elongation depends on fuel temperature and α_e goes in A) or is linked to the clad (fuel elongation depends on clad i.e. coolant temperature and α_e does not go in A). For metal fuel, linkage to the clad occurs after several atom percent burnup.

+In Fig. 1 and throughout this report several simplifying assumptions were made so as to remove design specific features and focus on size effects. These include neglecting control rod driveline and vessel wall thermal expansion.

performance, eg. A/B, $C\Delta T_c/B$, etc., reactivity coefficient data (i.e. the items in square brackets shown in Fig. 2) were drawn from a data base of reactor designs produced at ANL over the past four years which included roughly two dozen designs. These spanned a range from 400 to 3600 MWth, included oxide and metal fueled designs, homogeneous and radially heterogeneous layouts, core height from 36 to 40 inches, etc. The cores included here were all Pu (rather than U235) fueled. While this data base was less than fully consistent and had not been generated specifically for this purpose, it was at least consistent in the sense of all designs having been produced by the same design group using the same design philosophy and degree of aggressiveness, and using a fixed set of design codes and basic data.

Moreover, the methodology was to convert the reactivity coefficients (all at EOEC) to the α's defined in Fig. 2 using a common set of thermal and structural basic data as defined in Fig. 2 so as to isolate the reactor size effect. Thus, for example, in computing α_R the duct thermal expansion coefficient was always assumed to be that of HT-9 whereas in fact some of the designs had used D9; also for example, both drivers and internal blankets were included in the value of core Doppler, α_D; also in computing α_ℓ, the fuel was always assumed to be linked to the clad and the relevant thermal expansion coefficient was taken as that of HT-9.

The variations of the α's with reactor thermal rating which were thusly obtained are displayed in Figs. 3 through 7. Examination of these figures reaffirms the known relationships; for example Fig. 3 shows that the Doppler coefficient [¢/(°C in fuel)] is about two thirds as large in the harder-spectrum metal composition as compared to the oxide and that the values increase with reactor size as the enrichment decreases and the spectrum softens. Figures 4 and 5 display the more positive sodium density coefficient attendant the harder spectrum metal composition and the increase in its value with increasing reactor size as the neutron leakage fraction decreases. Also shown is the reduction in the positive sodium density coefficient which can be achieved by use of a radially heterogeneous layout to provide for internal leakage to absorptive media. Two sodium density coefficient curves are shown for the radially heterogeneous core layouts; one for sodium density worth in the driver only and one for driver plus internal blanket. The effective value for use in evaluating the asymptotic temperature rises should include the internal blanket and that is what is done here, -- while the contribution of sodium density to the prompt power coefficient would lie nearer to the driver only curve. Figures 6 and 7 show that the radial and axial expansion coefficients assuming the fuel is linked to the clad and that the duct and clad are both HT-9 are controlled by core dimensions and that the difference in composition between metal and oxide design plays no significant role.

All curves display strong core size dependencies for the α's in the 400 to 1500 MWth size range, but a much weaker size dependence from 1500 to 4000 MWth. It is of interest to note that for the sodium density coefficient the use of internal blankets can nearly totally arrest the increase in positive coefficient with core size which is seen for the homogeneous core layout -- an important point in that the positive sodium density coefficient works against the desired goal of large negative values of B and C to achieve passive shutdown.

(C) Trends of the Measurable Integral Reactivity Parameters A, B, and C with Reactor Size

The trend curves in the individual α's can be used to produce the trends versus reactor size of the integral reactivity parameters, A, B, and C, and their ratios which control passive reactivity shutdown performance. As with the α trend curves, the focus of this exercise is on isolating the size effect; therefore, uniformity of assumptions is important in computing A, B, and C. To that end, the formulas in Fig. 1 were used under the ground rules:

1) use the α trend curves in Figs. 3 through 7 (not specific data points),

2) use heterogeneous layout (not homogeneous) and use driver + internal blanket contributions to Na density and Doppler,

3) use fuel bonded to clad (not free of clad), -- so the α_ℓ term in A is zero in Fig. 1,

4) neglect difference between grid plate and above core load pad thermal expansion coefficient, neglect geometry factors, and neglect bowing, so that the same α_R is used to compute B and C as is shown in Fig. 1,

5) use HT-9 clad and grid plate (not austenitic steel),

6) neglect control rod driveline and vessel thermal expansion (which can be made small in zero burnup swing cores), and

7) assume size independent

ΔT_c = 150°C coolant temperature rise

$\overline{\Delta T_f}$ = 150°C metal fuel temperature rise (ave. fuel - ave. coolant)

750°C oxide temperature rise (ave. fuel - ave. coolant).

Because of the above simplifying assumptions, the trend curves should be viewed as generic and as representing a fuzzy zone; specific design selections -- such as core height (internal blanket/driver) ratio, austenitic v. ferritic duct material, etc. -- would move any specific reactor somewhat off the generic trend curve.

The trend curves of A, B, and C as generated by the above methodology are shown in Fig. 8. As with the trend curves of α, it is seen that a strong size dependence exists out to ~2000 MWth, but that for larger units the size dependence is weaker.

A is the product of the Doppler coefficient with the incremental temperature rise in the fuel pin relative to the coolant. The amplitude of A increases with reactor size for both metal and oxide cores because the Doppler becomes ever larger as the enrichment decreases and the spectrum softens.

Alternately, the amplitudes of B and C decrease with increasing reactor size for both oxide and metal cores. This is because both B and C are dominated by leakage related factors, and neutron leakage fraction diminishes with increasing reactor size. Specifically, radial and axial expansion effects become less negative the bigger the core, and these effects on the values of B and C are exacerbated because the negative leakage component of the overall positive sodium density coefficient becomes smaller the larger the core.

Perhaps the most striking feature of Fig. 8 is the dramatic difference in the value of A between oxide and metal core designs. Where does this come from?

- The ratio of Doppler coefficient itself remains near $1.6 = \frac{\alpha_D(\text{oxide})}{\alpha_D(\text{metal})}$, for all reactor sizes 500 MWth and larger (see Fig. 3).

- The ratio of incremental temperature rise in the fuel relative to the coolant is fixed at

$$\frac{\Delta T_f(\text{oxide})}{\Delta T_f(\text{metal})} = \frac{750^\circ C}{150^\circ C} = 5$$

for metal and oxide pins of the same heat rating as a result of the higher thermal conductivity of the metal fuel and use of a sodium bond.

These two components produce a constant factor of 8 larger A for the oxide cores as compared to metal cores at all core sizes larger than 500 MWth. This difference is the nub of the superior passive shutdown performance which is achievable by use of metal fuel. The value of A represents the reactivity (due to Doppler) which is vested in the incremental temperature rise of the fuel above the coolant. When the power is reduced to zero, the fuel pin incremental temperature rise collapses to zero and this reactivity is introduced as a positive reactivity; for oxide it gets to as much as $1.65 for larger reactor sizes whereas for metal it does not exceed about 20¢. For passive control, this positive reactivity must be compensated by a negative reactivity due to coolant temperature rise. The factor of eight smaller reactivity input provides an advantage for the metallic fueled systems.

Figure 9 shows the trend of power reactivity decrement, (A+B), and the relative size of its two components, A and B, versus reactor size. Since A stands for the reactivity vested in the incremental temperature rise of the fuel average above the coolant average while B stands for the reactivity vested in the average coolant temperature relative to the inlet coolant temperature, it is evident from the argument of the previous paragraph that passive shutdown is favored if the coolant's component, B, dominates the fuel's component, A, in the power reactivity decrement, (A+B). This favorable split in the makeup of the power reactivity decrement is achieved with metallic fuel and is not with oxide. A design strategy for reducing A without reducing B in the oxide case would be to reduce the heat rating. A factor of four derating (to ~3 kW/ft) would be sufficient to reduce A until it equaled B in the large oxide fueled cores.

To summarize, for both oxide and metal cores the trends in A, B, and C with reactor size are the same and are understandable: A becomes more negative and B and C become less negative as core size increases. Generally speaking these trends are unfavorable as regards passive reactivity shutdown performance. Further it is already clear that the factor of eight smaller reactivity vested in the fuel temperature rise in metal pins versus oxide is an advantage as regards passive shutdown performance. However, it is the ratios of A, B, and C which are enumerated in Eq. (3) which control the passive shutdown performance, so that the trends with size of these ratios are to be examined next.

IV) Trends in Passive Reactivity Shutdown with Reactor Size

Figure 10 displays two of the dimensionless ratios of integral reactivity parameters relevant to passive reactivity shutdown, A/B and $C\Delta T_c/B$, as computed using the A, B, and C trend curves of Fig. 9. Recall that sufficient (but not necessary) conditions for favorable passive reactivity shutdown include the conditions:

$A/B \leq 1$	for passive control of pump and BOP induced accident scenarios, eg. unprotected LOF, pump overspeed, LOHS, and chilled inlet.
$1 \leq \frac{C\Delta T_c}{B} \leq 2$	

Examination of the trend curve shows that for metal cores, favorable unprotected performance in pump and BOP induced accidents should be achievable in cores of the largest commercial size. Alternately, the sufficient conditions are not met in oxide cores of modular size or larger. Figure 11 makes this point more directly by using the expressions for asymptotic δT_{out} which are found in Table I. The asymptotic outlet temperature increases remain below the materials limits for metal cores whereas for oxide cores the LOHS is a problem already at about 500 MWth and the LOF is a problem above about 2000 MWth.

While remaining in an acceptable range, the asymptotic outlet temperature increase suffered in a LOF in metal cores does somewhat increase as the reactor size grows to the 3500 to 4000 MWth range. Thus as the asymptote increases it may be desirable to reduce the relative overshoot. The short-time peak overshoot of the outlet temperature over and above its asymptotic value is minimized by designing for a pump coastdown time (τ) relative to the time constant of delayed neutron hold back of power decay ($1/\lambda$) such that the quantity

$$\tau\lambda(1 + A/B)^2 \, |B| > 1\$.$$

Thus, the value vs. reactor size of the quantity

$$\tau^* = \frac{1\$}{|B|} \frac{1}{(1+A/B)^2} \frac{1}{\lambda}$$

which is equal to the shortest pump coastdown time for which the inequality is met is of interest. Using the data from the previous several figures it can be shown that τ^* is invariant with reactor size and has a value of about 14 sec*.

Trend curves have not been generated for the rod runout TOP passive shutdown performance for which the requirement is:

$$\frac{\Delta\rho_{TOP}}{|B|} = \left(\frac{\text{Burnup Control Swing}}{\text{No. of Primary Rods}}\right)\left(\text{1st rod out interaction factor}\right)\frac{1}{|B|} \leq 1$$

because most of the core designs in the data base had not exploited design options which were available to reduce burnup control swing. However, it is clear that the larger the core, the easier it is to achieve a zero burnup control swing design because the enrichment is reduced as leakage fraction is lowered. And, in the case of metal-fueled cores where internal breeding benefits from a hard neutron spectrum and a high heavy metal density fuel form, zero burnup swing designs have been developed in both the small modular size range[1] for SAFR and PRISM as well as at the LSPB size of 3500 MWth[5]. Moreover, the longer migration length attendant the hard spectrum of the metallic core designs somewhat retards the increase in rod interaction factor with increasing core size. Thus, it is known that passive reactivity control of slow TOP's should be achievable in metal core sizes from the modular to the largest commercial size.

Oxide cores designed to achieve favorable passive LOF and LOHS shutdown performance at any size will likely be derated, will become substantially larger, and the enrichment will thereby be substantially reduced in any case -- trends in the right direction for reducing burnup control swing and improving TOP passive shutdown performance as well. This design solution has a technical disadvantage in that the much lower enrichment will give rise to a much increased fluence to burnup ratio at discharge which, for currently available structural materials, may reduce the allowable discharge burnup to a rather low level. However, for the oxide cores, detailed studies have not as yet been performed by us to see what is actually achievable.

V) Trends vs. Reactor Size in Potential for Reduced Reliance on Control Rods for Reactor Control

As is discussed above, design for favorable passive shutdown performance leads to a core that is designed with a high internal conversion ratio, a small burnup control swing and thus, a beginning of cycle reactivity excess which is relatively small compared to the reactivity vested in the incremental temperature rise of the coolant average above the inlet temperature, i.e.

$$\frac{\Delta\rho_{TOP}}{|B|} < 1 \quad \text{(see Eqs. (3) and (2)).}$$

---

*Here λ is taken as 12 sec^{-1}.

Further, the core is designed such that the reactivity vested in the coolant temperature rise dominates that vested in the fuel temperature rise i.e.

$A/B < 1$ (see Eq. (3).

Such a core -- designed so that the reactivity vested in coolant temperature changes is large when compared both to that reactivity vested in beginning of cycle excess reactivity and to that reactivity vested in power changes -- such a core offers the potential for operational control on coolant temperature as opposed to controlling on control rod position[6]. Three options can be considered; control on inlet temperature, control on pump speed; or combined control on both.

In a rough way (neglecting nonlinearities) the power reactivity decrement, (A+B) can be identified with a slow power coefficient of reactivity at constant flow and inlet temperature:

$$(A+B) = \frac{\text{¢}}{(100\% \text{ increase in power})} \Bigg|_{\text{constant flow, } T_{in}}.$$

Similarly, C, can be identified with (indeed is) an inlet temperature coefficient of reactivity at constant flow and constant power:

$$C = \frac{\text{¢}}{1^{0}\text{C increase in inlet temperature}} \Bigg|_{\text{constant flow, power}},$$

and, with a sign change, B can be identified with a flow coefficient of reactivity at constant inlet temperature and power:

$$-B = \frac{\text{¢}}{(100\% \text{ increase in flow})} \Bigg|_{\text{constant inlet temperature, power}}.$$

Thus, the low frequency gain of a pump speed controller and inlet temperature controller of reactor power can be roughly approximated by:

$$G_{pump}(W=0) = \frac{B}{A+B} = \frac{\% \text{ change in power}}{\% \text{ change in flow}} \Bigg|_{\text{constant } T_{inlet}}, \quad (4)$$

$$G_{T_{inlet}}(W=0) = \frac{100\ C}{A+B} = \frac{\% \text{ change in power}}{^{0}\text{C change in } T_{inlet}} \Bigg|_{\text{constant flow}}. \quad (5)$$

If the pump and inlet temperature are used together to control at constant core ΔT_c, the zero frequency gain is:

$$G_{both}(W=0) = \frac{100\ C}{A} = \frac{\% \text{ change in power}}{^{0}\text{C change in } T_{inlet}} \Bigg|_{\text{constant } \Delta T_c}.$$

For the U.S. modular sized reactors which are designed for passive shutdown using metal fuel, the values of these gains suggest the potential for using flow or inlet temperature control[6] to reduce reliance on control rods; eg. using the values from Fig. 8 at 1000 MWth:

$$\frac{1}{G_{pump}(0)} = \text{\% change in flow to achieve a 1\% change in power at constant } T_{inlet}$$

$$= 1.35\%,$$

$$\frac{1}{G_{T_{inlet}}(0)} = {}^{o}C \text{ change in } T_{inlet} \text{ to achieve a 1\% change in power at constant pump speed}$$

$$= 1.85^{o}C,$$

$$\frac{1}{G_{both}(0)} = {}^{o}C \text{ change in } T_{inlet} \text{ to achieve a 1\% change in power at constant } \Delta T_c$$

$$= 0.48^{o}C.$$

The combined control, G_{both}, requires a smaller inlet temperature change to effect a given power change than is the case when pump speed is held constant because in the former case the inlet temperature change need not overcome the reactivity introduced by the resultant power/flow change whereas in the latter case it must*.

The potential for control on pump speed or inlet temperature or a combination on U.S. modular sized plants is under investigation, both experimentally at EBR-II[7] and analytically[8] in support of SAFR and PRISM accounting for the higher frequency dependencies of G_{pump} and $G_{T_{inlet}}$ and their coupling with the time constants of the primary heat transport system and the BOP. It is of interest to investigate how such control schemes could be extended to larger sized plants, should they prove to be feasible at the modular size. In that regard, Fig. 9 displays a fascinating distinction between metal and oxide trends versus size -- in metal cores, the power reactivity decrement, (A+B) -- i.e. the denominator of the controller gains -- decreases with size whereas in oxide cores it increases+. This is in contrast to B and C -- the numerators of the controller gains -- which always decrease with size irrespective of fuel type. As a result, for oxide cores, the controller gains relevant to inherent control, G_{pump}, $G_{T_{inlet}}$, and G_{both}, become dramatically less favorable as core size is increased because the power coefficient grows while the flow and inlet temperature coefficients diminish. In contrast, for metal cores, the power coefficient decreases with

---

*If this seems confusing, set P/F = 1 in Eq. (1), linearize, and solve for $\delta P/\delta T_{in}$.

+Mathematically this is a direct consequence of A growing, B decreasing, and A dominating B in oxide cores while the reverse is true for metal.

size in keeping with the similar decreases in flow and inlet temperature coefficients, B and C; and as a result the gains do not deteriorate as quickly with size.

Figure 12 which displays the trends of $G^{-1}_{pump}(0)$, $G^{-1}_{T_{inlet}}(0)$, and $G^{-1}_{both}(0)$ with reactor size, shows that even at 4000 MWth a 1% change in flow, or a 2.5°C change in inlet temperature at constant pump speed, or a 1°C change in inlet temperature at constant core ΔT_c in a metal core is large enough to change power by 1%. Gains in this range -- 3 to 4 times larger than attainable in oxide cores -- suggest the extendability of reduced reliance on control rods in metal cores to the largest commercial size should the approach prove to be attractive in development of the U.S. modular sized plants.

VI) Conclusions

Favorable passive reactivity shutdown performance in response to unprotected accidents initiators has been shown to be achievable when the measurable, integral reactivity parameters:

(A+B)	power reactivity decrement (proportional to power coefficient of reactivity)
B	component due to coolant temperature rise (proportional to flow coefficient of reactivity)
C	inlet temperature coefficient of reactivity
$\Delta\rho_{TOP}$	single rod runout TOP initiator (proportional to burnup control swing)
τ	pump coastdown time constant

satisfy the requirements:

A, B, C	all negative

$$A/B \leq 1$$

$$\Delta\rho_{TOP}/|B| \leq 1$$

$$1 \leq \frac{C\Delta T_c}{B} \leq 2$$

$$\tau\lambda(1 + A/B)^2|B| > 1\$.$$

The trends in these dimensionless ratios with reactor size for both oxide and metal fuel have been developed based on a data base of about two dozen reactor designs in the range 400 to 3600 MWth. The results are shown in Figs. 8 through 11.

Based on the results displayed in the figures, it is shown that favorable passive reactivity shutdown performance is achievable even in the largest commercial sized reactors (~3600 to 4000 MWth) by use of the metal fuel form.

Favorable passive reactivity shutdown performance may be possible with the oxide fuel form by means of derating by factors of up to 4 (for large commercial sizes) so as to suitably reduce the Doppler reactivity which is vested in the incremental temperature rise of the fuel above that of the coolant. Evaluation of the impact on discharge fluence/burnup ratio for the resultant larger, derated, lower-enrichment core is known to be unfavorable, but has not as yet been specifically evaluated. Evaluation of the economic impacts of the resultant larger initial heavy metal and fissile masses and the larger vessel size is beyond the scope of this physics investigation.

As a different facet of the same trends, it is seen that in metal cores the potential is retained to the largest commercial core sizes to reduce reliance on control rods by using pump speed or inlet temperature for operational control. This happens because the reactivity vested in coolant temperature changes is large relative to that vested in the initial excess reactivity (related to burnup swing) and in the incremental rise in temperature of the fuel relative to the coolant (related to the power coefficient).

In this study a number of simplifying approximations were made in order to isolate the size effect using a diverse data base not generated for that specific purpose. Thus, any given reactor design could be expected to deviate to some degree from the trend curves developed here as a consequence of specific design selections. Examples of design selections which are available to impact the results are linear heat rating, pump coastdown time constant, internal blanket to driver ratio, core height, selection of ferritic or austenitic steel for the ducts and grid plate, UIS and core support geometry and coolant flow paths -- which affect control rod driveline and vessel expansion feedback reactivities -- and etc. Thus, the trend curves developed and discussed here provide a general overview of what should be feasible and what is out of the question in extending passive shutdown performance established for modular designs to large cores, but the detailed performance will depend on the detailed design.

The general conclusion is that the favorable passive reactivity control features which accrue to the metallic-fueled reactors in the modular size range can be achieved as well in the larger commercial sizes.

References

1. D. C. Wade and Y. I. Chang, "The Integral Fast Reactor (IFR) Concept: Physics of Operation and Safety," Proc. Int'l. Topical Meeting on Advances in Reactor Physics Mathematics and Computation, Paris, Vol. 1, p. 311, April 1987.

2. D. R. Pedersen, personal communication, Argonne National Laboratory (1987).

3. Rößback, Broadley, Cinotti and Hofmann, "Status of Optimization of the Decay Heat Removal System of the SNR-2".

4. R. H. Sevy, personal communication, Argonne National Laboratory (1985).

5. Y. Orechwa, S. T. Yang, and R. B. Turski, personal communication, Argonne National Laboratory (1987).

6. H. P. Planchon, J. I. Sackett, G. H. Golden and R. H. Sevy, "Implications of the EBR-II Inherent Safety Demonstration Test," Nuclear Engineering and Design, 101, pp. 75-90 (1987).

7. J. I. Sackett and H. P. Planchon, personal communication, Argonne National Laboratory (1987).

8. T. Wei, personal communication, Argonne National Laboratory (1987).

TABLE I. Quasi Static Reactivity Balance Results for Unprotected Accidents

	Asymptotic State				Intermediate State	Indicated Trend for Inherent Shutdown*	
	P	F	δT_{in}	δT_{out}			
LOHS	~0	1	$\frac{A+B}{C}$	$\left(\frac{1+A/B}{\frac{C\Delta T_c}{B}} - 1\right)\Delta T_c$	Monotonic transition to asymptotic	• A+B small • C large	
TOP	~1 (after rise in T_{in} due to BOP heat removal limit)	1	$\frac{\Delta\rho_{TOP}}{-C}$	$\delta T_{out} = \delta T_{in}$ $= \left(\frac{\Delta\rho_{TOP}/B}{-C\Delta T_c/B}\right)\Delta T_c$	Initial rise at constant T_{in} $P = 1 + \frac{-\Delta\rho_{TOP}/B}{1 + A/B}$ $\delta T_{cut} = \left(\frac{-\Delta\rho_{TOP}/B}{1 + A/B}\right)\Delta T_c$	• A+B large • C large • $\Delta\rho_{TOP}$ small	
LOF	~0	Natural Circulation	0	$(A/B)\Delta T_c$	overshoot relative to delayed neutron hold-back of power decay minimized if $\lambda\tau(1+A/B)^2\lvert B\rvert >> 1$	• A small • B large • τ long	
Chilled Inlet	$1 - \frac{C\delta T_{in}}{A+B}$	1	$\lvert-\delta T_{in}\rvert \leq (T_{inlet} - T_{Na\ freeze})$ $\approx 1.5\ \Delta T_c$	$\left(\frac{C\Delta T_c/B}{1 + A/B} - 1\right)(-\delta T_{in})$	monotonic transition	• C small • A+B large	
Pump Overspeed	$\frac{1 + A/B}{1/F + A/B}$ (always > 1)	F>1	0	$\left(\frac{1}{1 + \frac{A/B}{1+A/B}(F-1)}\right)\Delta T_c$ (always < 0)	monotonic transition	• A negative • B negative	

*Conflicts are seen to exist between desirable trends for different ATWS events. Resolution of these conflicts is discussed in the text.

Components of Power and Power/Flow Reactivity Decrements and of T_{inlet} Coefficient of Reactivity

A (ϕ) =	α_D +	0 bounded to clad α_ℓ free of clad				* $\overline{\Delta T_f}$ (ave. fuel - ave. coolant) temperature
B (ϕ) =	α_D +	α_ℓ	+ α_{Na} +	$2\alpha_R$		* $\frac{\Delta T_c}{2}$ (ave. coolant-T_{inlet}) temperature
C (ϕ/°C) =	α_D +	α_ℓ	+ α_{Na} +	α_R		
	Doppler	Fuel axial expansion	Na density	Radial expansion		
Typical Size ϕ/°C	-0.05 to -0.1	-0.1	+0.15 to 0.2	-0.2 to 0.3		
	Associated with fuel temperature	?	Associated with coolant temperature			

Fig. 1

$\alpha_D = \left[T \frac{dk}{dT}\right] \frac{1}{\beta} \frac{1}{\bar{T}_f}$ — Doppler (¢/°C) — negative

$\alpha_\ell = \left[\frac{dk}{dH}\right]_{\substack{\text{mass} \\ \text{const.}}} \frac{1}{\beta} H \alpha$ ← Linear Coeff of Expansion — Fuel Axial Expansion (¢/°C) — negative

$17.6 \cdot 10^{-6}$	Metal Fuel
19 or $20 \cdot 10^{-6}$	Austenitic Clad
$12.8 \cdot 10^{-6}$	Oxide Fuel
$13.9 \cdot 10^{-6}$	Ferritic Clad

$\alpha_{Na} = \left[\frac{dk}{dNa}\right] \frac{1}{\beta} \left(\frac{1}{\rho} \frac{d\rho}{dT}\right)$ ← volumetric coeff of expansion $0.281 \cdot 10^{-3}$/°C — Na Density (¢/°C) — positive

$\alpha_R = \left[\frac{dk}{dR}\right]_{\substack{\text{mass} \\ \text{const}}} \frac{1}{\beta} R \alpha$ ← linear coeff of expansion; ← core/blk equivalent radius — Core Radial Expansion (¢/°C) — negative

Physics Input: $\left[\ \right]_\beta$

Here

R = radius of core/radial blanket interface.

H = core height.

$\overline{T_f}$ = average fuel temperature $\simeq T_{in} + \frac{\Delta T_c}{2} + \overline{\Delta T_f}$.

$\overline{\Delta T_f}$ = increment in average fuel temperature relative to average coolant temperature $\simeq \begin{cases} 150 \text{ metal} \\ 750 \text{ oxide} \end{cases}$ at $-12 \frac{kW}{ft}$.

ΔT_c = coolant temperature rise $\simeq 150$°C

Fig. 2

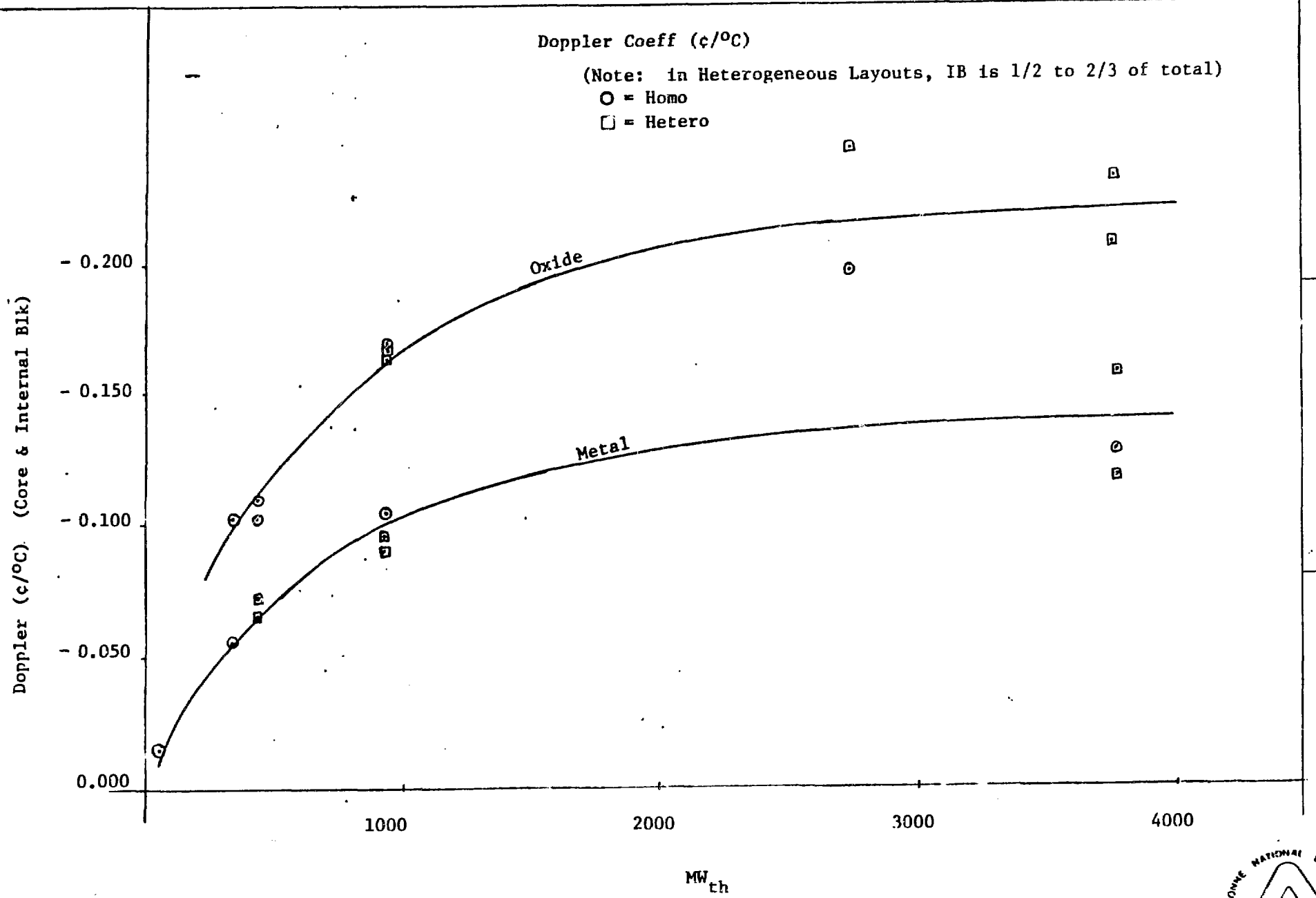

Fig. 3

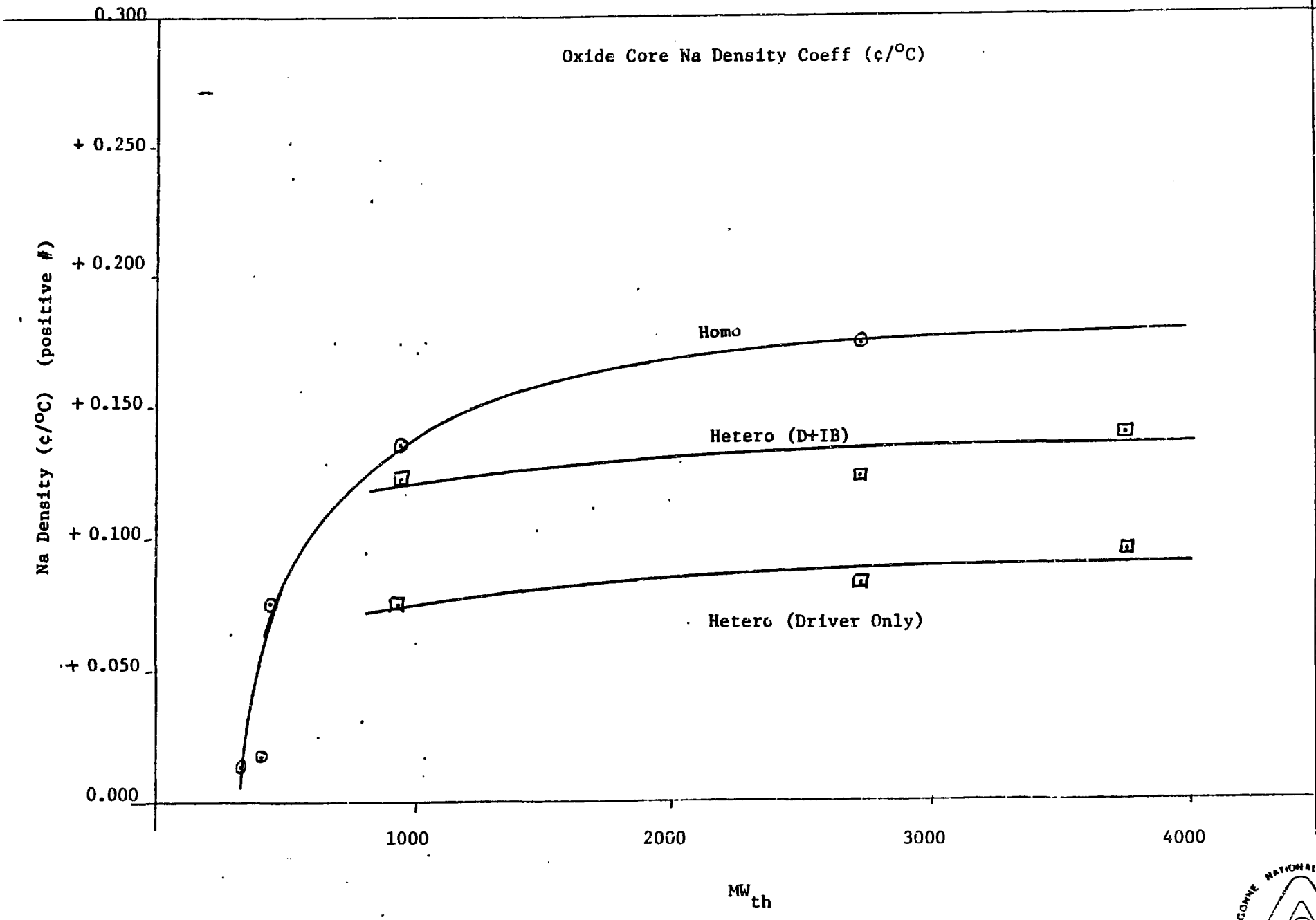
Oxide Core Na Density Coeff (¢/°C)
Na Density (¢/°C) (positive #)
0.300
+ 0.250
+ 0.200
+ 0.150
+ 0.100
+ 0.050
0.000
Homo
Hetero (D+IB)
Hetero (Driver Only)
1000
2000
3000
4000
MW th

Fig. 4

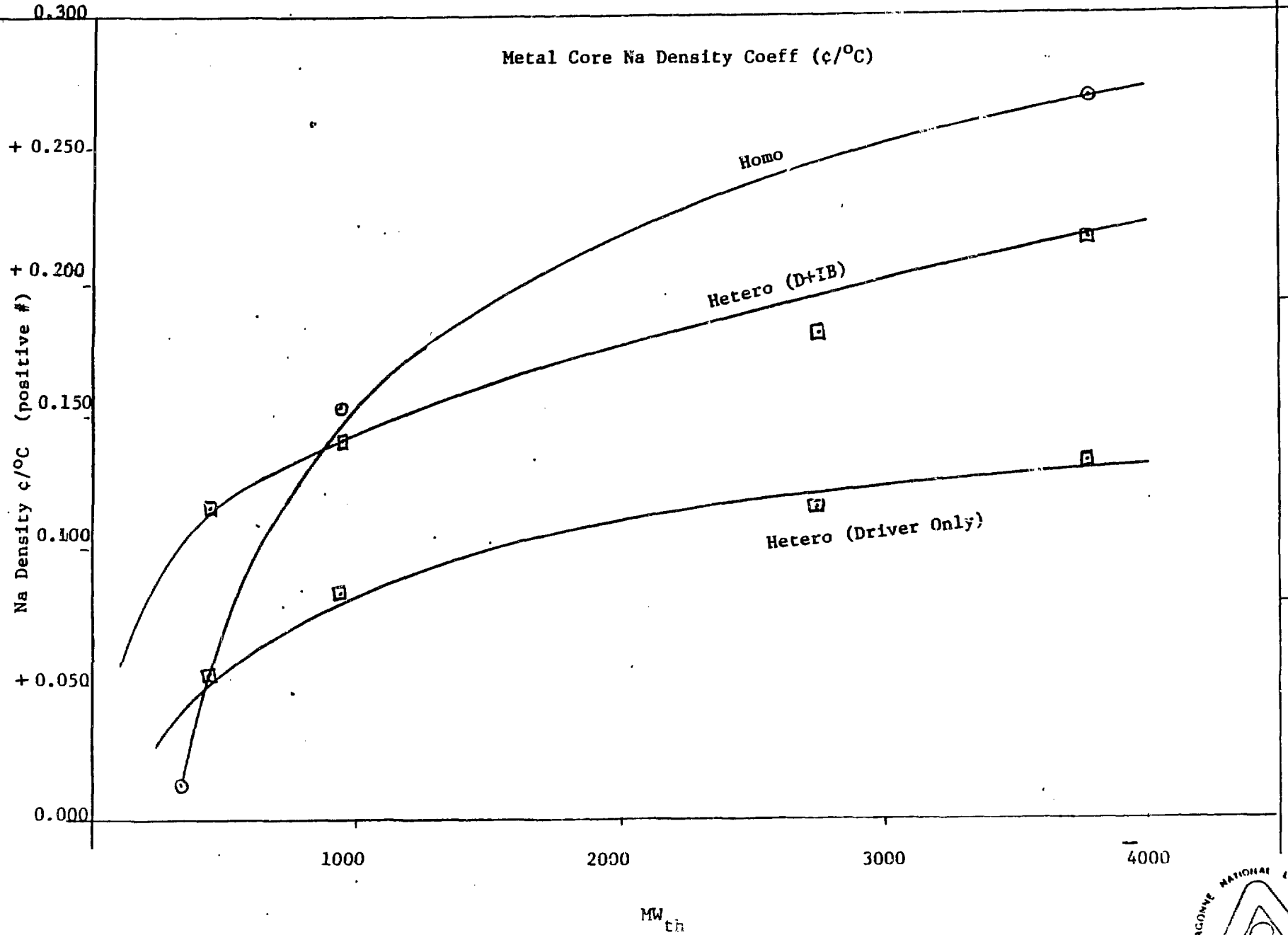
Metal Core Na Density Coeff (¢/°C)
Homo
Hetero (D+IB)
Hetero (Driver Only)
Na Density ¢/°C (positive #)
0.300
+ 0.250
+ 0.200
0.150
0.100
+ 0.050
0.000
1000
2000
3000
4000
MW th

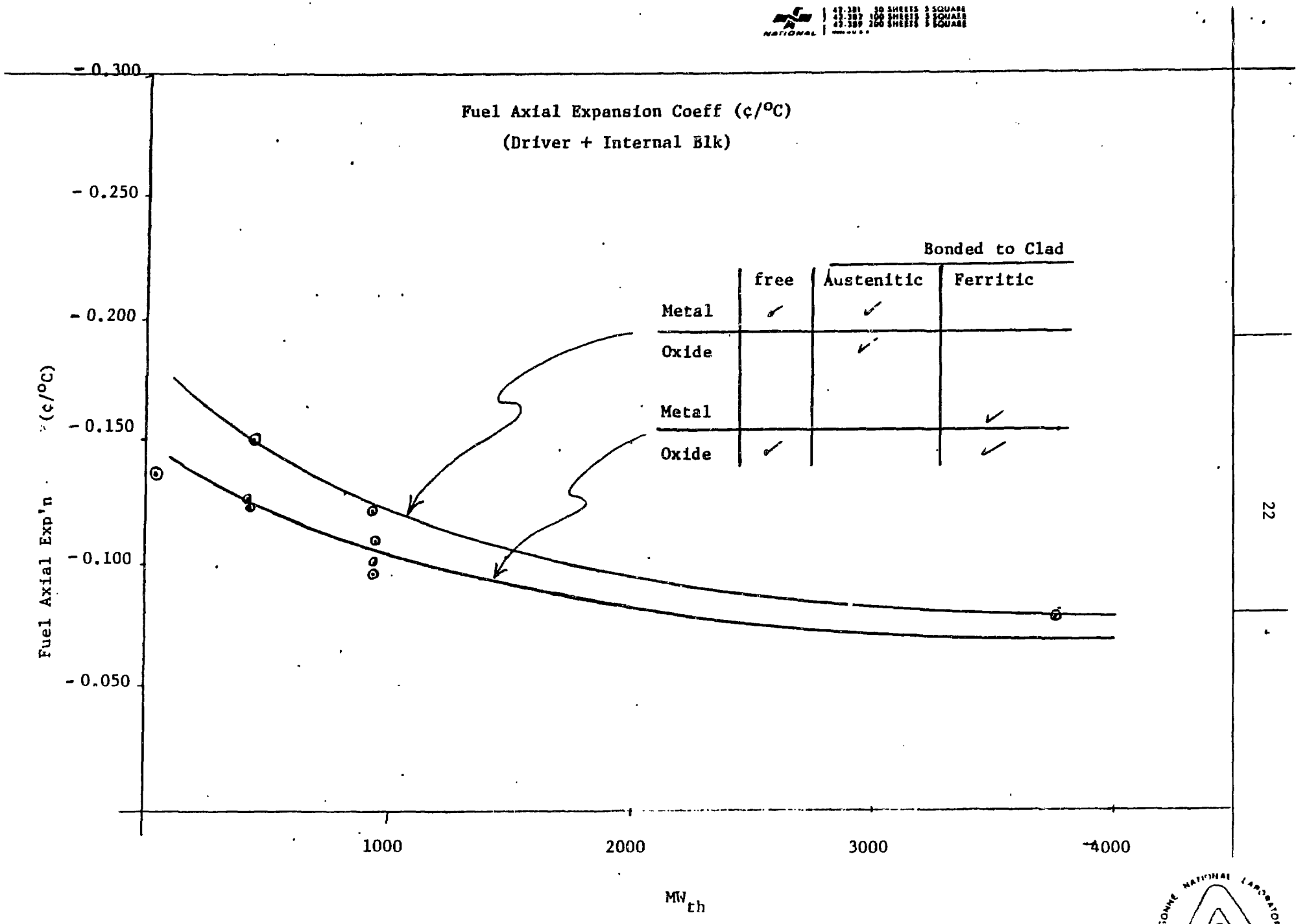
Fuel Axial Expansion Coeff (¢/°C)
(Driver + Internal Blk)
Bonded to Clad
free
Austenitic
Ferritic
Metal
Oxide
Metal
Oxide
- 0.300
- 0.250
- 0.200
- 0.150
- 0.100
- 0.050
Fuel Axial Exp'n (¢/°C)
1000
2000
3000
4000
MW th

Fig. 6

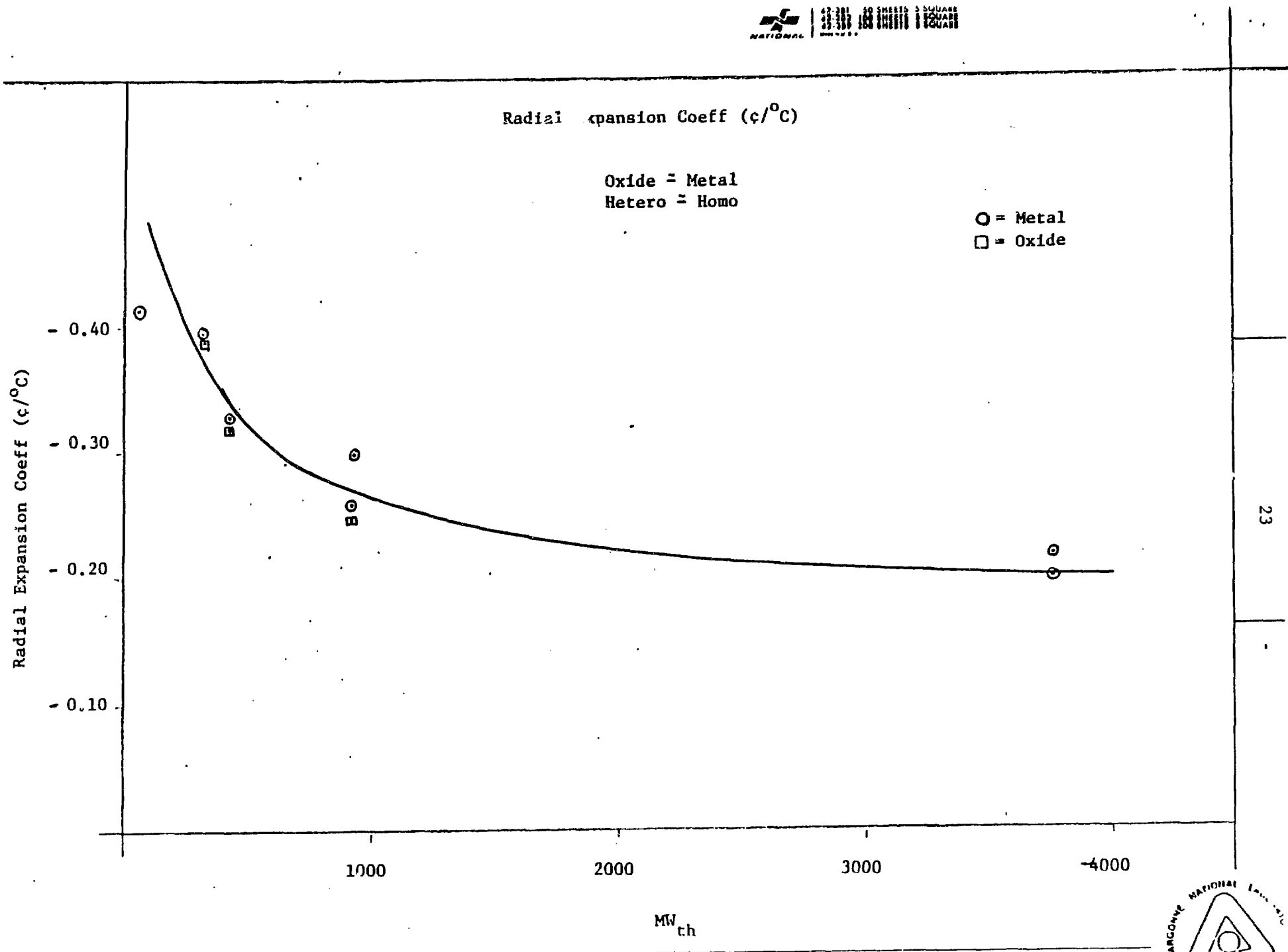
Radial Expansion Coeff (¢/°C)
Oxide = Metal
Hetero = Homo
O = Metal
□ = Oxide
Radial Expansion Coeff (¢/°C)
0.40
0.30
0.20
0.10
1000
2000
3000
4000
MW th

Fig. 7

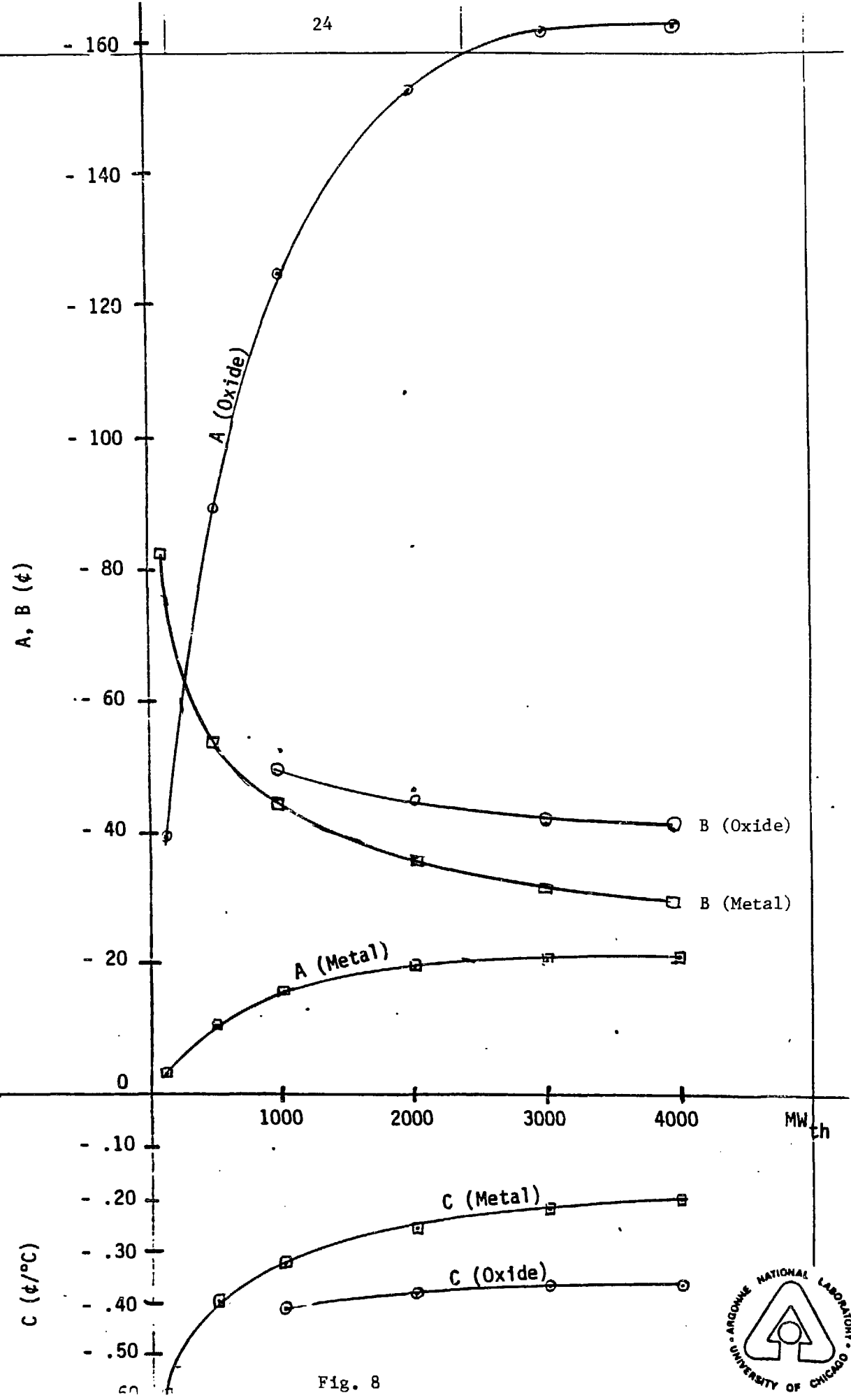
- 160
- 140
- 120
- 100
- 80
- 60
- 40
- 20
0
A, B (¢)
A (Oxide)
B (Oxide)
B (Metal)
A (Metal)
1000
2000
3000
4000
MWth
- .10
- .20
- .30
- .40
- .50
C (¢/°C)
C (Metal)
C (Oxide)

Fig. 8

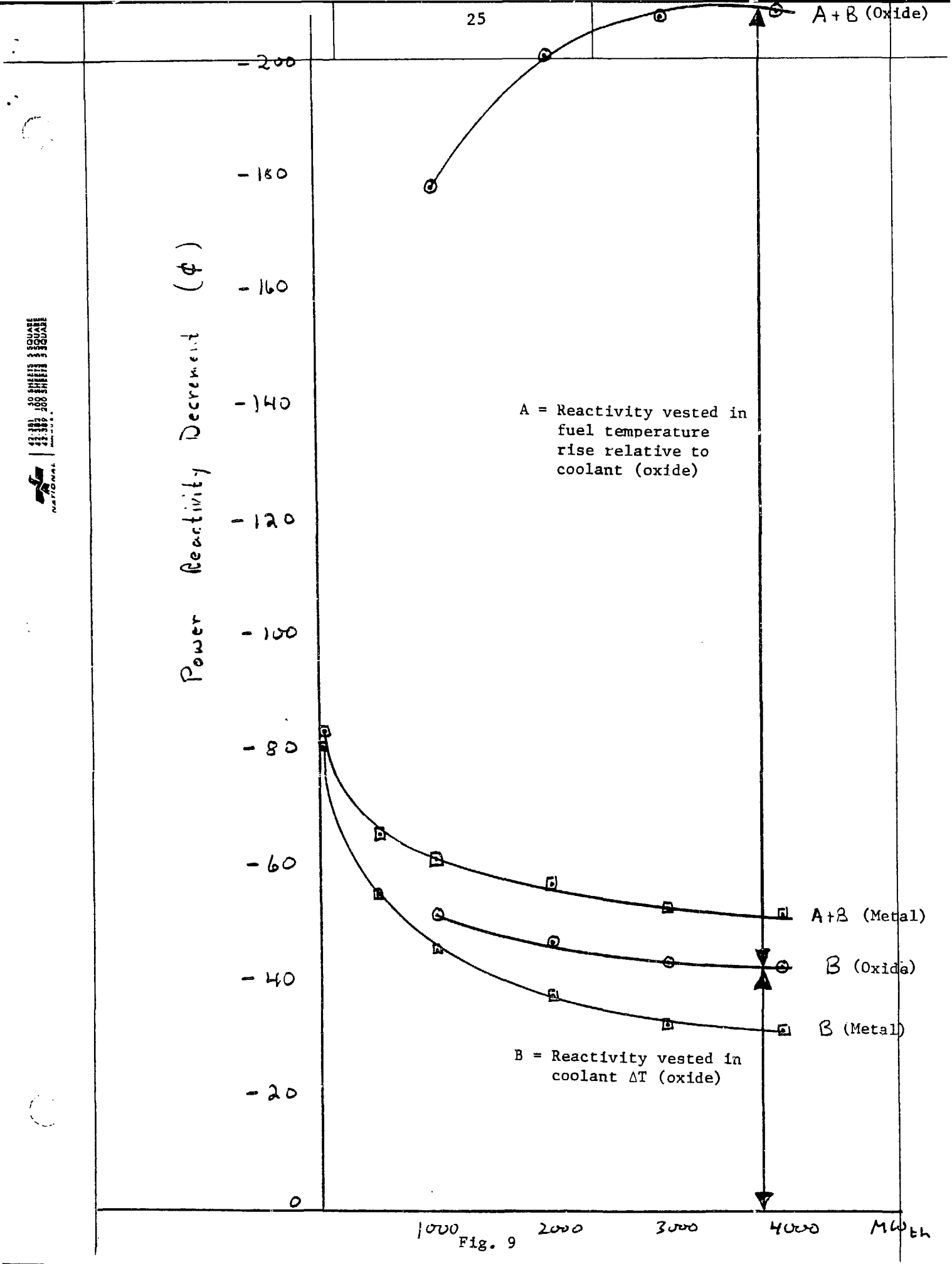
A + B (Oxide)
-200
-180
-160
-140
-120
-100
-80
-60
-40
-20
0
Power Reactivity Decrement (¢)
A = Reactivity vested in fuel temperature rise relative to coolant (oxide)
A+B (Metal)
B (Oxide)
B (Metal)
B = Reactivity vested in coolant ΔT (oxide)
1000
2000
3000
4000
MWth

Fig. 9

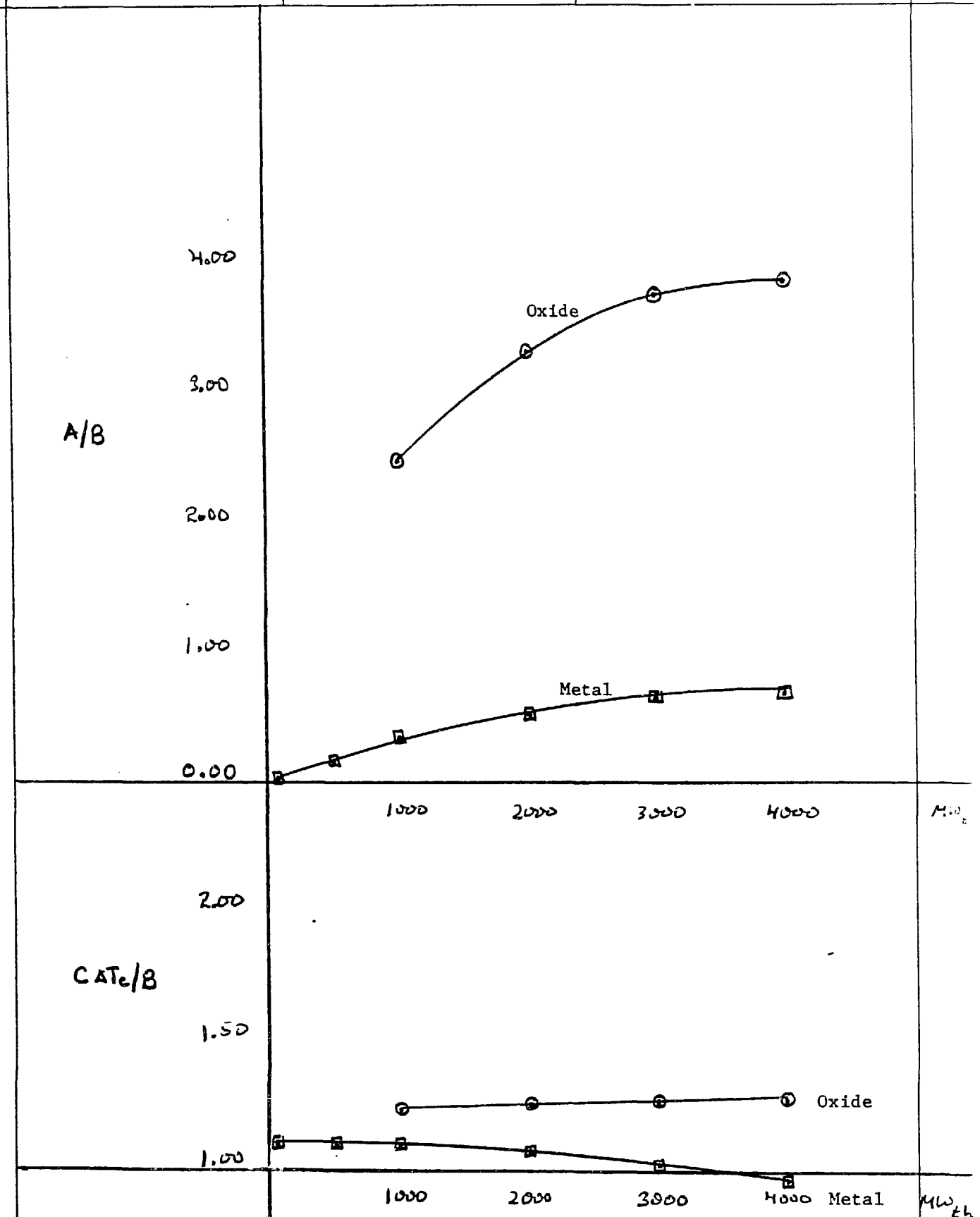
4.00
3.00
A/B
2.00
1.00
0.00
Oxide
Metal
1000
2000
3000
4000
2.00
CΔTc/B
1.50
1.00
Oxide
Metal
1000
2000
3000
4000

Fig. 10

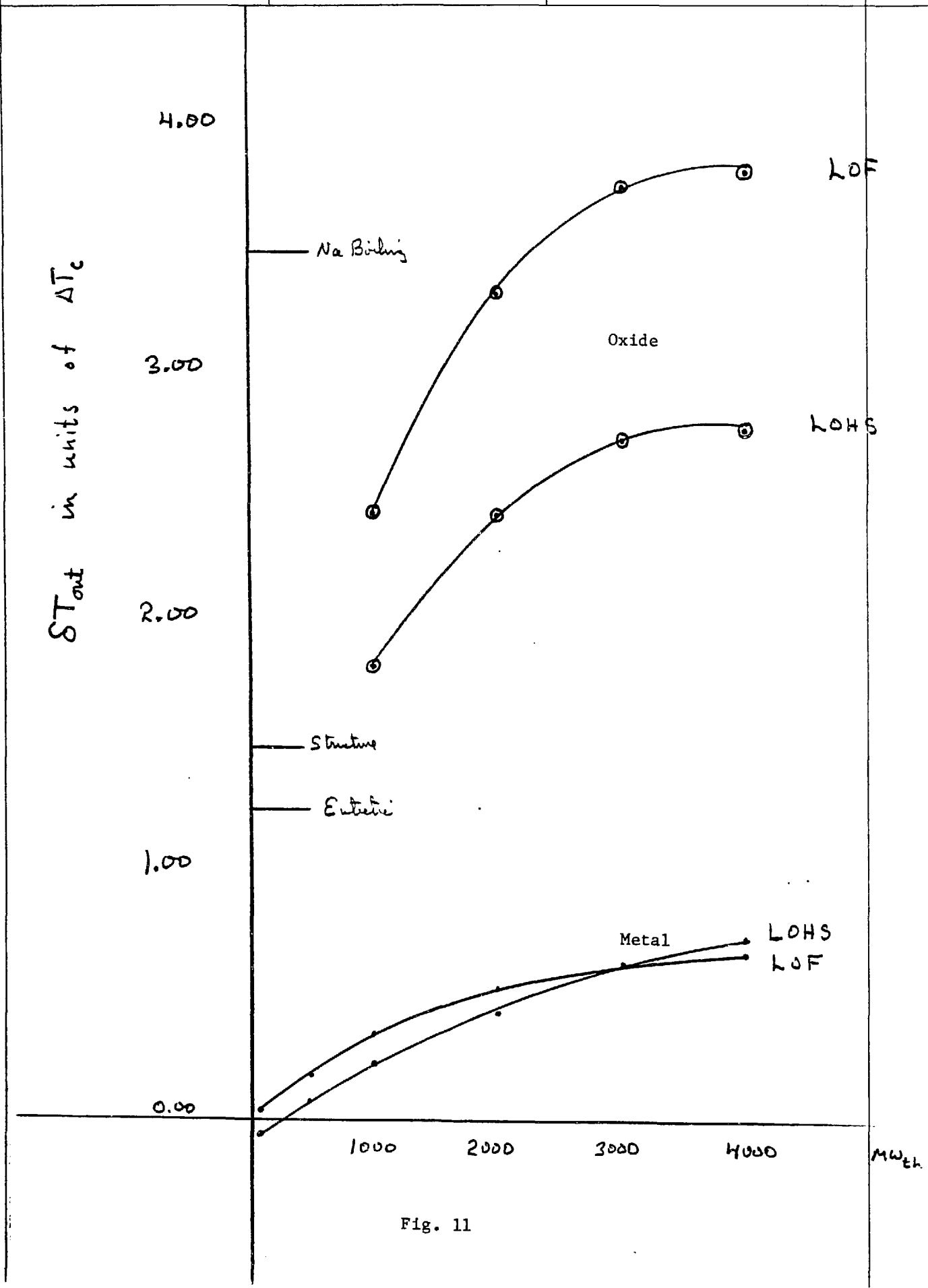
4.00
3.00
2.00
1.00
0.00
δT_{out} in units of ΔT_c
Na Boiling
Structure
Eutectic
LOF
Oxide
LOHS
Metal
LOHS
LOF
1000
2000
3000
4000
MW$_{th}$

Fig. 11

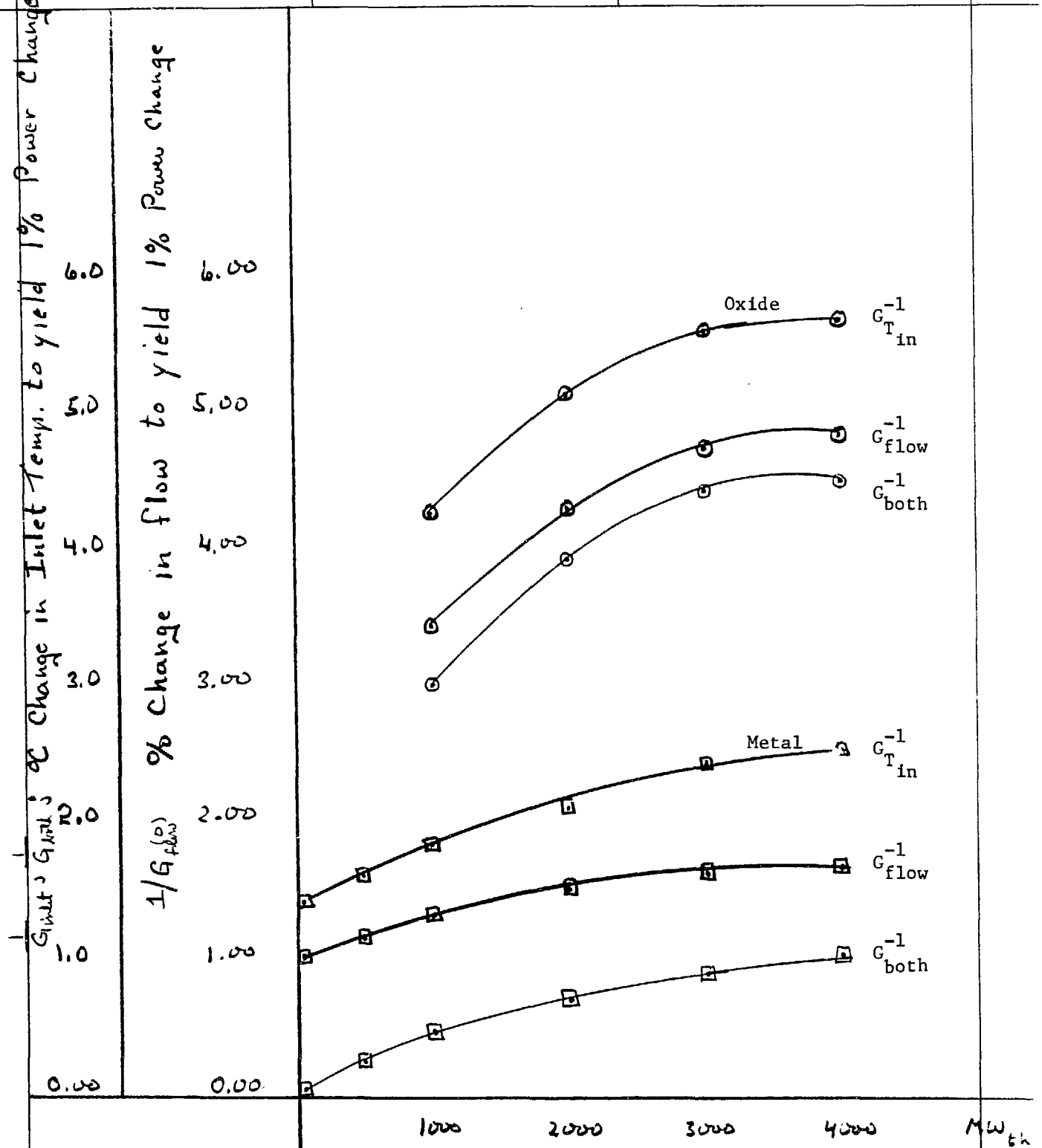
Oxide
$G_{T_{in}}^{-1}$
G_{flow}^{-1}
G_{both}^{-1}
Metal
$G_{T_{in}}^{-1}$
G_{flow}^{-1}
G_{both}^{-1}
1000
2000
3000
4000
MW_{th}
$1/G_{flow}^{(0)}$ % Change in flow to yield 1% Power Change
G_{inlet}^{-1} % Change in Inlet Temp. to yield 1% Power Change
6.00
5.00
4.00
3.00
2.00
1.00
0.00
6.0
5.0
4.0
3.0
2.0
1.0
0.0

Fig. 12

DISCLAIMER